



# A preparative small-molecule mimic of liver CYP450 enzymes in the aliphatic C-H oxidation of carbocyclic N-heterocycles

Rachel K. Chambers<sup>a</sup> 📵, Jacob D. Weaver<sup>a</sup> 📵, Jinho Kim<sup>a</sup> 📵, Jason L. Hoar<sup>b</sup> 📵, Shane W. Krska<sup>b</sup> 📵, and M. Christina White<sup>a,1</sup> 📵

Edited by Marcetta Darensbourg, Texas A&M University, College Station, TX; received January 6, 2023; accepted May 15, 2023

An emerging trend in small-molecule pharmaceuticals, generally composed of nitrogen heterocycles (N-heterocycles), is the incorporation of aliphatic fragments. Derivatization of the aliphatic fragments to improve drug properties or identify metabolites often requires lengthy de novo syntheses. Cytochrome P450 (CYP450) enzymes are capable of direct site- and chemo-selective oxidation of a broad range of substrates but are not preparative. A chemoinformatic analysis underscored limited structural diversity of N-heterocyclic substrates oxidized using chemical methods relative to pharmaceutical chemical space. Here, we describe a preparative chemical method for direct aliphatic oxidation that tolerates a wide range of nitrogen functionality (chemoselective) and matches the site of oxidation (site-selective) of liver CYP450 enzymes. Commercial small-molecule catalyst Mn(CF<sub>3</sub>-PDP) selectively effects direct methylene oxidation in compounds bearing 25 distinct heterocycles including 14 out of 27 of the most frequent N-heterocycles found in U.S. Food and Drug Administration (FDA)-approved drugs. Mn(CF<sub>3</sub>-PDP) oxidations of carbocyclic bioisostere drug candidates (for example, HCV NS5B and COX-2 inhibitors including valdecoxib and celecoxib derivatives) and precursors of antipsychotic drugs blonanserin, buspirone, and tiospirone and the fungicide penconazole are demonstrated to match the major site of aliphatic metabolism obtained with liver microsomes. Oxidations are demonstrated at low Mn(CF<sub>3</sub>-PDP) loadings (2.5 to 5 mol%) on gram scales of substrate to furnish preparative amounts of oxidized products. A chemoinformatic analysis supports that Mn(CF<sub>3</sub>-PDP) significantly expands the pharmaceutical chemical space accessible to small-molecule C-H oxidation catalysis.

C-H activation | oxidation | bioisosteres | metabolism | CYP450 mimic

Nitrogen-containing heterocycles are present in 59% of FDA-approved pharmaceuticals (1). An emerging trend for such N-heterocyclic drugs is the incorporation of small, methylene-rich carbocycles as a way to improve their potency and solubility (Fig. 1A) (2, 3). However, structure-activity relationships (SAR) and metabolite identification (MetID) studies are more challenging with these molecules relative to their aryl counterparts (Fig. 1B) (4). Functionality at methylene sites is generally incorporated via lengthy de novo syntheses due to the nonpreparative nature of biotransformations (5, 6) and the sparsity of chemical methods for such chemoselective oxidations (7, 8) (Fig. 1 C and D) (9–11).

Small-molecule catalysis has long held promise for mimicking nature's enzymes in effecting remote hydroxylations of unactivated C-H bonds (12-16). Whereas cytochrome P450 (CYP450) enzymes involved in biosynthesis of natural products are generally substrate-specific, those involved in metabolism of xenobiotics are more promiscuous (17, 18). Despite significant structural differences, studies of iron and manganese PDP aliphatic C-H oxidation catalysis have illuminated functional and mechanistic similarities with heme and nonheme iron oxidation enzymes (19, 20). Only recently has this interesting reactivity been rendered selective and preparative in complex molecule settings (21-24). Among the challenges that remain are those pertaining to chemoselectivity, that is oxidizing strong bonds (ca. 96 to 98 kcal/mol, pK<sub>a</sub> ~ 50) in the presence of other oxidatively labile functionality (for example,  $\pi$ -systems, nitrogen) routinely found in biologically relevant molecules (25).

PDP catalysis has been demonstrated to selectively oxidize molecules from every natural product class and emerging classes of pharmaceuticals (24, 26). Selectivity without specificity is attributed to PDP catalysis' ability to distinguish between ubiquitous aliphatic C-H bonds on the basis of their electronic, steric, and stereoelectronic properties rather than by topologically specific catalyst-substrate interactions (21, 22). The switch from iron to manganese furnished PDP catalysts (26-28) that can selectively oxidize aliphatic sites in the presence of aromatic functionality (26, 28). Moreover, PDP catalysts have been shown to be compatible with  $HBF_4$  (pK<sub>a</sub> ~ -0.4) protonation of amines that strongly deactivates nitrogen toward direct or alpha oxidation and enables remote methylene oxidation (29). Herein, we reveal that commercial Mn(CF<sub>3</sub>-PDP)

## Significance

C-H oxidation reactions are rarely used in laboratory synthesis because without a directing group on the substrate, they lack the selectivity and reactivity to preparatively furnish mono-oxidized products. Here, we report that commercial Mn(CF<sub>3</sub>-PDP) catalyst promotes nondirected methylene C-H oxidations with exceptional tolerance for oxidatively labile nitrogen heterocycles abundant in pharmaceuticals. Site selectivities match those of the major metabolites from promiscuous liver cytochrome P450 (CYP450) enzymes. Direct gram-scale syntheses of drug metabolites and derivatives are demonstrated that otherwise required de novo syntheses. Chemoinformatic analysis guided and quantitatively evaluated this and other methods' capacity to oxidize substrates in smallmolecule pharmaceutical space and underscores the tremendous potential of Mn(CF<sub>3</sub>-PDP) as a functional CYP450 enzyme mimic in pharmaceutical studies.

Author contributions: R.K.C., J.D.W., S.W.K., and M.C.W. designed research; R.K.C., J.D.W., J.K., and J.L.H. performed research; R.K.C., J.D.W., J.K., J.L.H., S.W.K., and M.C.W. analyzed data; and R.K.C., J.D.W., and M.C.W. wrote the paper.

Competing interest statement: The University of Illinois has filed a patent application (number 16/569,492) on the Mn(CF3-PDP) catalyst that lists M.C.W. as an inventor.

This article is a PNAS Direct Submission.

Copyright © 2023 the Author(s). Published by PNAS. This article is distributed under Creative Commons Attribution-NonCommercial-NoDerivatives License 4.0

<sup>1</sup>To whom correspondence may be addressed. Email: mcwhite7@illinois.edu.

This article contains supporting information online at https://www.pnas.org/lookup/suppl/doi:10.1073/ pnas.2300315120/-/DCSupplemental.

Published July 10, 2023.

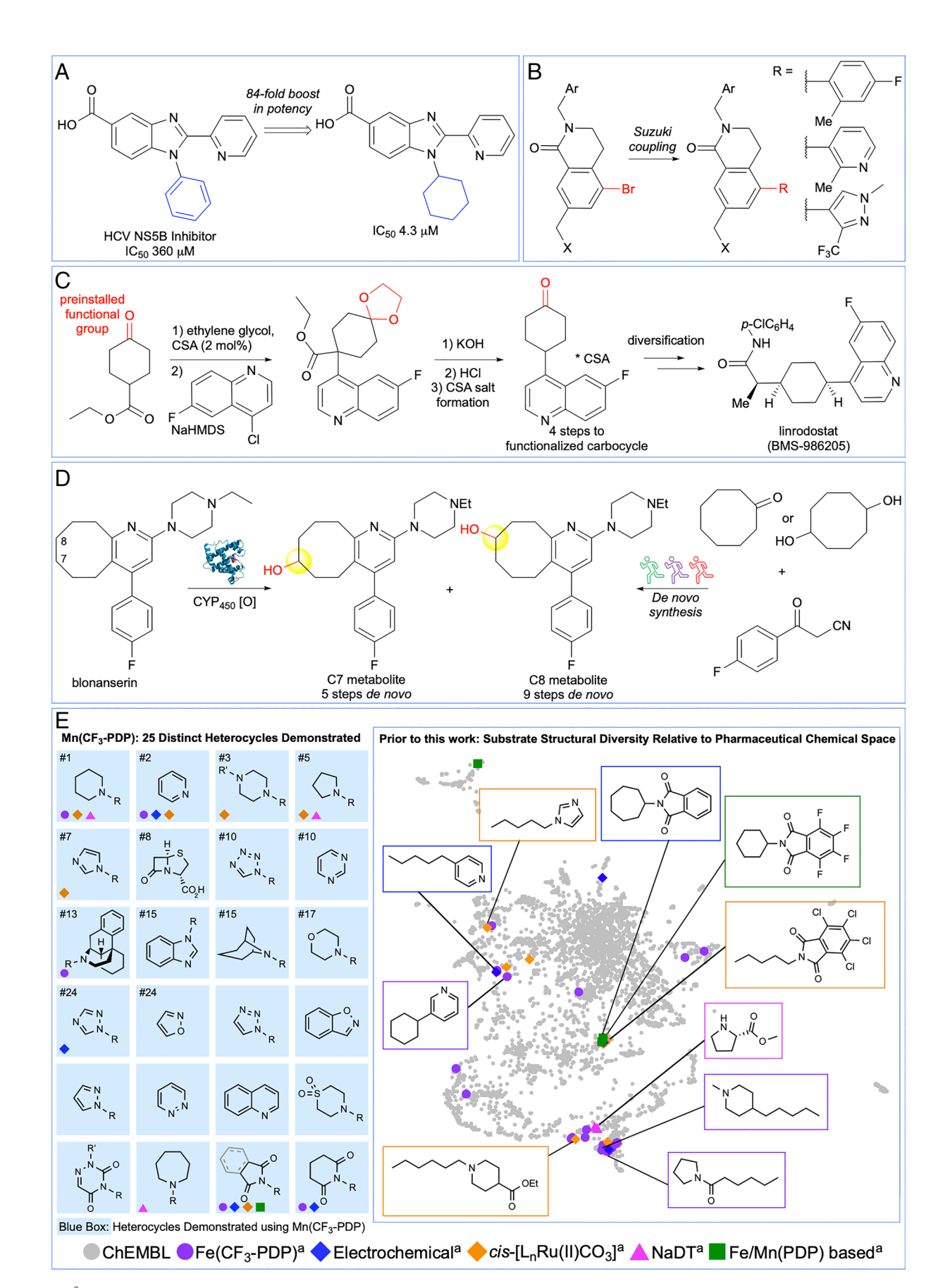


**Fig. 1.**  $C(sp^3)$ -H oxidation in the presence of *N*-heterocyclic functionality. (*A*) Saturated carbocycles are bioisosteres of aryl fragments and can improve the potency and solubility of *N*-heterocyclic drugs. (*B*) In contrast to carbocycles, aryl fragments in *N*-heterocyclic drugs are rapidly diversified. (*C*) Multistep syntheses are often required to introduce oxygen functionality onto carbocycles in *N*-heterocyclic drugs. (*D*) 5 to 9 step de novo syntheses were required to access aliphatic metabolites of the antipsychotic drug blonanserin. (*E*) Previously reported methylene C-H oxidation methods demonstrate limited heterocycle scope and structural diversity in comparison to pharmaceutical chemical space. <sup>a</sup>These catalysts can be found in references.

catalyst 1 used in combination with an HBF<sub>4</sub> protonation strategy enables a chemical methylene C-H oxidation method that is applicable to a broad range of nitrogen heterocycles (25 distinct heterocycles), operates on preparative scales, and matches the site selectivities of liver CYP450 enzymes (Fig. 1*E*).

#### **Results and Discussion**

Metal catalysts and dioxirane oxidants, often in combination with fluorinated solvents or Brønsted acid additives, have demonstrated  $C(sp^3)$ –H oxidations in the presence of oxidizable functionality (for example, alcohols, amides, and some Nheterocycles); however, this chemoselectivity has generally been limited to 3° and benzylic oxidations (30–35). An initial evaluation of heterocycle scope diversity for methylene C-H oxidation methods reported from 2015 to 2021 showed very limited scope (7 out of 27 of the top heterocycles in FDA-approved drugs, 26%, Fig. 1*E*) (29, 36–42). Moreover, visualization of the substrate scope of these methods relative to pharmaceutical chemical space showed clustering in sparsely populated areas indicating a lack of both substrate diversity and drug-likeness (Fig. 1E, vide infra). We first systematically evaluated commercial Mn(CF<sub>3</sub>-PDP) 1 methylene oxidations on small cycloalkanes containing N-heterocycles with pK<sub>aH</sub>'s (i.e., pK<sub>a</sub> of the conjugate acid) spanning the broadest range reported to date (approximately 11.2 to -3.0, see *SI Appendix* for heterocycle pK<sub>aH</sub> references, Fig. 2*A*). Using Mn(CF<sub>3</sub>-PDP) 1 catalysis with the HBF<sub>4</sub> protonation strategy, saturated nitrogen heterocycles (pK<sub>aH</sub> ca. 11.2 to 10.3) including pyrrolidine, piperidine, and tropane as well as tertiary amines, such as N-methylbenzylamines, afford remote oxidation predictably at the most sterically exposed, electron-rich methylene site in preparative yields (3, 4, 7, 8) (21, 22). Mn(CF<sub>3</sub>-PDP) 1 oxidations operate under acidic conditions (26) (chloroacetic acid additive, p $K_a \sim 2.7$ ), and remote oxidation products could be observed in some cases without HBF<sub>4</sub> protection. The diminished yields and significant recovered starting material (rsm) observed in these cases are consistent with catalyst deactivation: upon amine protonation, chloroacetate anion may interfere with oxidation.

Saturated heterocycles with multiple sites available for C-H oxidation are challenging substrates and have been sparsely evaluated for selective methylene oxidation (39). Overoxidation was observed on the heterocyclic ring of an HBF<sub>4</sub>-protected azepane substrate (30% mono-oxidation 5 and 40% dioxidation S41, see *SI Appendix*), demonstrating that nitrogen protonation does not stop oxidation on the azepane core (Fig. 2A). Upon decreasing the catalyst, oxidant, and acid loadings [2.5 mol% Mn(CF<sub>3</sub>-PDP) 1, 7.5 equiv. ClAcOH, and 5 equiv.  $H_2O_2$ ], preparative amounts of remote mono-oxidized azepane product 5 could be obtained (50% mono-oxidation **5** and 20% dioxidation **S41**). Alternatively, HBF<sub>4</sub> protonation of a benzylated azepane halts benzylic and alpha N-oxidation while allowing for C3 heterocycle oxidation to afford 6. In heterocycles containing multiple heteroatoms whose lone pair electrons may hyperconjugatively activate adjacent  $C(sp^3)$ -H bonds toward oxidation, we examined whether HBF<sub>4</sub> protonation of the basic nitrogen could inductively deactivate the entire heterocycle from Mn(CF<sub>3</sub>-PDP) oxidation. N-trifluoroacetyl-protected piperazine and morpholines underwent remote aliphatic oxidations under these conditions (9, 10, and 11, respectively). Interestingly, protonated amine functionality in morpholine affords selectivity at the most electron-rich δ-site on the cyclohexyl ring. Typically, little selectivity between the  $\delta$ - and  $\gamma$ -sites is observed due to competing stereoelectronic effects (relief of ring strain) that favor the  $\gamma$ -site (vide infra, 14

to 16 and 18) (22). Despite an electronically withdrawing sulfone in a thiomorpholine dioxide substrate, HBF4 protonation was required for productive remote oxidation to 13.

Analogous to observations with basic saturated heterocycles, basic aromatic heterocycles such as imidazole and pyridine (pK<sub>aH</sub> ca. 6.9 and 5.2), also require HBF<sub>4</sub> protonation to afford remote methylene oxidation products (Fig. 2A). Imidazole 12 was furnished in comparable efficiency at 2.5 mol% Mn(CF<sub>3</sub>-PDP) 1 and higher mass balance relative to the 10 mol% Mn(CF<sub>3</sub>-PDP) 1 conditions (SI Appendix), representing among the lowest catalyst loadings reported to date for methylene oxidation and projecting practical utility for multigram scale reactions (vide infra) (39, 41, 42). Cyclohexanone-substituted pyridines are extensively derivatized scaffolds in the synthesis of biologically active molecules. Oxidation of 4-cyclohexyl pyridine afforded both γ- and δ-ketones 14 in synthetically useful yield with reduced functional group manipulations relative to prior syntheses (SI Appendix) (43).

Tolerance for heterocycles with increased aza-substitution has rarely been demonstrated by previous methylene oxidation methods. Cyclohexyl-pyridazines and -pyrimidine all afforded preparative yields of remote oxidized products 15, 16, and 18 under HBF<sub>4</sub> protonation (Fig. 2A). Interestingly, cyclohexylpyrimidine was found to proceed in good yields without protonation, likely a result of diminished heterocycle basicity from the inductive withdrawal of additional nitrogen atoms (44). In contrast, pyridazine-containing compounds underwent decomposition without HBF<sub>4</sub> protonation, possibly due to increased nucleophilicity of the adjacent nitrogen atoms resulting from lone pair repulsion (α-effect) (44). 1,2,4- and 1,2,3-triazoles afford remote oxidation products 17 and 19 in significantly improved yields upon protonation.

For heterocycles having a pK<sub>aH</sub> below 0, the addition of HBF<sub>4</sub> is not beneficial to Mn(CF<sub>3</sub>-PDP) **1** C-H oxidation (*SI Appendix*). Tetrazole, a common bioisostere for carboxylic acids (45), underwent remote 2° oxidation in synthetically useful yield only without HBF<sub>4</sub> protonation (20, Fig. 2A). Isoxazoles are privileged scaffolds present in pharmaceuticals such as parecoxib and valdecoxib (46). Although a modest yield of the desired remote 2° C-H oxidation product 21 is isolated for a monosubstituted isoxazole, a trisubstituted isoxazole affords significantly improved yield (vide infra). As has been observed with other oxidants (37-39, 41), electron-deficient phthalimide heterocycles are well tolerated and afford preparative yields of remote oxidized product 22. Consistent with what we noted above for azepane 5, the lower catalyst loading conditions significantly improves mass balance of 22, likely due to a decrease in overoxidation on the cycloheptane ring. Average chemoselectivity (2° C–H oxidation products/conversion) for this reaction is 59% (±15%). In many cases, intractable mixtures of polar side products were noted likely due to overoxidation of the heterocyclic cores.

Manganese PDP-based catalysis in acidic, fluorinated alcohol solvents enables chemoselective tertiary (3°) C-H hydroxylations in N-heterocyclic substrates via hydrogen-bonding deactivation of nitrogen (32, 34). We questioned whether the suprastoichiometric chloroacetic acid additive could facilitate Mn(PDP) 2 3° C-H hydroxylations in heterocyclic substrates across a pK<sub>3H</sub> range of 10.3 to 1.2 (Fig. 2B). In contrast to remote methylene oxidations, 3° oxidation is observed for all heterocycles in this pK<sub>aH</sub> range without HBF<sub>4</sub> protonation, albeit in lower yields (23 to 30). Reduction in the concentration of active catalyst via chloroacetate anion and/or free amine likely does not significantly impact yields of lower-energy C-H bond oxidations. This is consistent with previous observations that 3° and alpha to nitrogen C-H hydroxylations proceed with larger heterocycle scope and often reduced catalyst loadings (0.1 to 0.5 mol%) relative to more energetically challenging methylene oxidations (28, 31, 47).

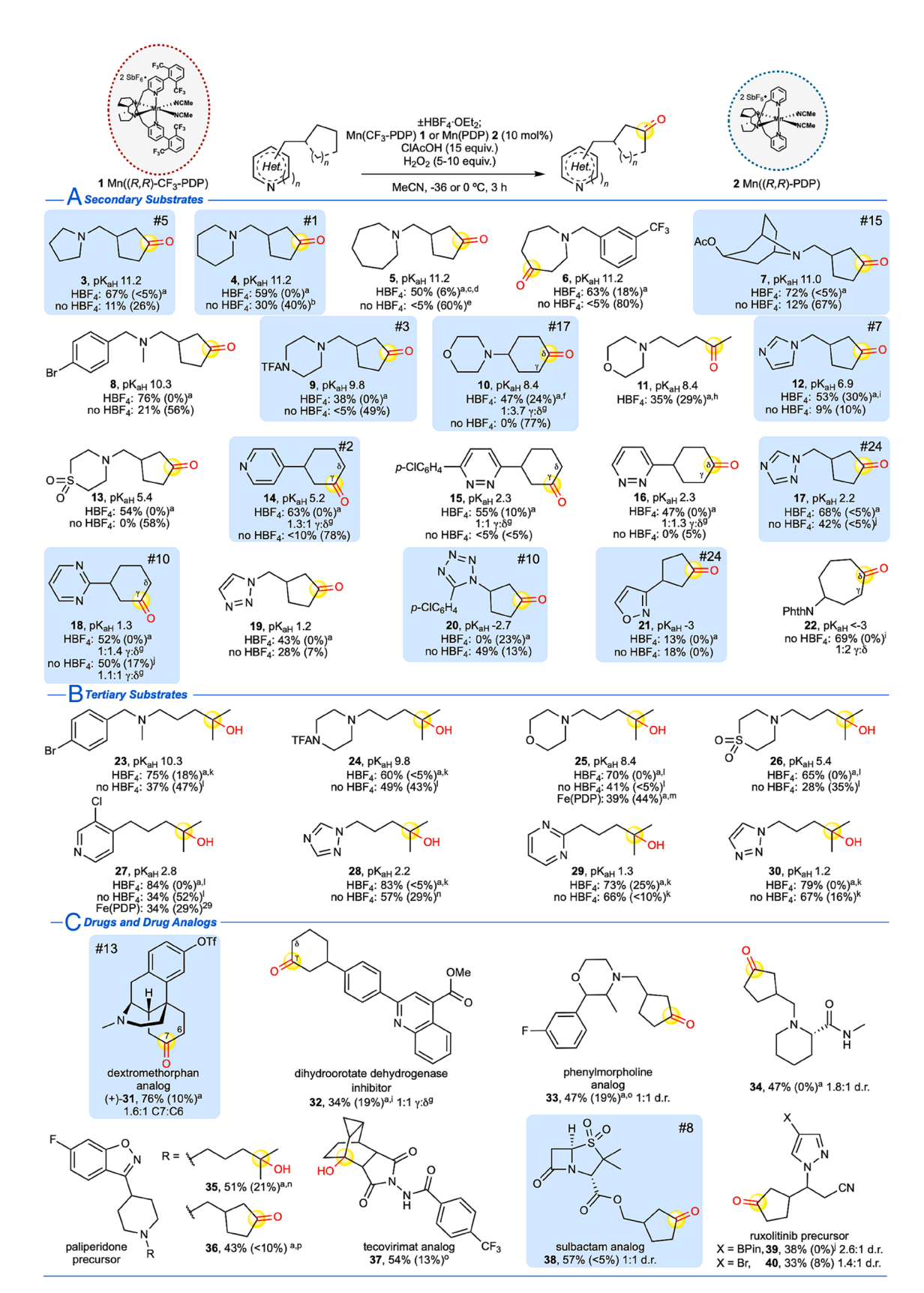


Fig. 2. *N*-heterocycle scope of (A) Mn(CF<sub>3</sub>-PDP) **1** methylene C–H oxidation and (*B*) Mn(PDP) **2** tertiary C–H oxidations with and without HBF4 nitrogen protonation. (C) Aliphatic C–H oxidation of drugs and drug derivatives with and without HBF<sub>4</sub> nitrogen protonation. Isolated yields are an average of two to three experiments, major isolated site of oxidation is highlighted in yellow, and recovered starting material (RSM) is given in parentheses. Experimental pK<sub>aH</sub> reported in water (see *SI Appendix* for references). Blue boxes with numbers indicate frequency of *N*-heterocycles in FDA approved drugs according to ref. 1. CIAcOH, chloroacetic acid. NPhth, phthalimide. General methylene oxidation with HBF<sub>4</sub> was done using Method A at -36 °C unless otherwise noted. General methylene oxidation without HBF<sub>4</sub> was done using Method B unless otherwise noted. <sup>8</sup>Nitrogen was HBF<sub>4</sub>\*OEt<sub>2</sub> protected as described in Materials and Methods. <sup>8</sup>Method A at 0 °C. <sup>6</sup>Modified Method D [2.5 mol% Mn(CF<sub>3</sub>-PDP) **1**, 7.5 equiv. CIAcOH, 5 equiv. H<sub>2</sub>O<sub>2</sub>] at -36 °C. <sup>6</sup>With 20% di-oxidation. <sup>8</sup>Modified Method D [2.5 mol% Mn(CF<sub>3</sub>-PDP) **1**] at 0 °C. <sup>6</sup>Ratios are statistically corrected. <sup>8</sup>Method C [3 x 5 mol% Mn(CF<sub>3</sub>-PDP) **1**] at 0 °C. <sup>6</sup>Method D. <sup>1</sup>Method A at -36 °C. <sup>6</sup>Method B with Mn(PDP) **2**. <sup>1</sup>Method C [3 x 5 mol% Mn(CF<sub>3</sub>-PDP) **1**] at -36 °C. <sup>8</sup>Method B. <sup>8</sup>Method C [3 x 5 mol% Mn(CF<sub>3</sub>-PDP) **1**] at -36 °C. <sup>8</sup>Method B. <sup>9</sup>Method B. <sup>9</sup>Method C [3 x 5 mol% Mn(CF<sub>3</sub>-PDP) **1**] at -36 °C. <sup>8</sup>Method B. <sup>9</sup>Method C [3 x 5 mol% Mn(CF<sub>3</sub>-PDP) **1**] at -36 °C. <sup>8</sup>Method B. <sup>9</sup>Method C [3 x 5 mol% Mn(CF<sub>3</sub>-PDP) **1**] at -36 °C. <sup>8</sup>Method B. <sup>9</sup>Method C [3 x 5 mol% Mn(CF<sub>3</sub>-PDP) **1**] at -36 °C. <sup>8</sup>Method B. <sup>9</sup>Method C [3 x 5 mol% Mn(CF<sub>3</sub>-PDP) **1**] at -36 °C. <sup>8</sup>Method C [3 x 5 mol% Mn(CF<sub>3</sub>-PDP) **1**] at -36 °C. <sup>8</sup>Method C [3 x 5 mol% Mn(CF<sub>3</sub>-PDP) **1**] at -36 °C. <sup>8</sup>Method C [3 x 5 mol% Mn(CF<sub>3</sub>-PDP) **1**] at -36 °C. <sup>8</sup>Method C [3 x 5 mol% Mn(CF<sub>3</sub>-PDP) **1**] at -36 °C. <sup>8</sup>Method C [3 x 5 mol% Mn(CF<sub>3</sub>-PDP) **1**] at -36

Having delineated heterocycle scope within simple substrates of low complexity [Figs. 2A, general index of molecular complexity = BertzCT (48) = 96 to 527],  $Mn(CF_3-PDP)$  1 remote oxidations were evaluated in pharmaceutically relevant small molecules containing heterocycles and/or nitrogen motifs of increasing complexity (Fig. 2C, BertzCT = 236 to 924). A dextromethorphan derivative, containing an oxidatively labile morphinan core, previously underwent Fe(CF<sub>3</sub>-PDP) methylene oxidation with HBF<sub>4</sub> protonation in 45% yield (29), whereas (*R*,*R*)-Mn(CF<sub>3</sub>-PDP) 1 catalysis afforded significantly improved chemoselectivity to afford 76% overall yield of remote ketone products (+)-31a (C7) and **31b** (C6), as well as C6 alcohol (+)-**31c** (1.6:1 = C7:C6, see SI Appendix). A dihydroorotate dehydrogenase inhibitor (49) bearing a quinoline moiety afforded remote methylene oxidation products 32 in a modest 21% yield under standard conditions (SI Appendix), likely due to the presence of an oxidatively labile aromatic ring. Employing the lower catalyst loading conditions (2.5 mol%), an improvement in yield to 34% was observed.

Heterocycles with multiple heteroatoms proceeded with predictable chemoselectivities in more complex molecule settings (Fig. 2C). A phenylmorpholine analog (50) bearing a doubly activated benzylic/ethereal 3° C-H bond afforded remote methylene oxidation on the cyclopentyl ring in good yield (33, 47%). Piperidine carboxamide, a substructure found in bupivacaine, a local anesthetic agent, underwent Mn(CF<sub>3</sub>-PDP) 1 remote oxidation on a cyclopentyl ring in 47% yield (34). Although amide motifs generally require a separate imidate protection (36), piperidine HBF<sub>4</sub> protonation likely inductively deactivates the adjacent amide to enable remote methylene oxidation. Benzisoxazoles are privileged structures in medicinal chemistry (51). Derivatives of the antipsychotic drug paliperidone containing a piperidylbenzisoxazole core underwent Mn(PDP) 2 and Mn(CF<sub>3</sub>-PDP) 1 remote 3° and 2° C-H oxidations in 51% and 43% yield, respectively (35 and 36). Underscoring the challenge of generating functionalized carbocycles, traditional installation of the oxidized methanecyclopentane fragment onto these heterocycles required a seven-step de novo synthesis from prefunctionalized starting material (SI Appendix) (52).

Electron-deficient heterocycles generally do not benefit from HBF<sub>4</sub> protonation prior to remote C-H oxidation (Fig. 2C). Saturated tecovirimat (53), an antipox viral drug featuring a polycyclic hydrocarbon skeleton and an electron-deficient N-benzoamido moiety, underwent Mn(CF<sub>3</sub>-PDP) 1 hydroxylation at the sterically exposed 3° C-H bond in 54% yield with no observed opening of the adjacent cyclopropane (37). An analog of the antibiotic sulbactam, bearing a prevalent  $\beta$ -lactam core flanked by two strongly electron-withdrawing groups, afforded remote methylene oxidation product 38 in 57% yield. As described above, heterocycles with a pK<sub>aH</sub> >1 should benefit from HBF<sub>4</sub> protonation; however, pyrazole heterocycles having a pK<sub>aH</sub> of ca. 2.5 afforded rsm or decomposition upon HBF<sub>4</sub> protection/oxidation (SI Appendix). For example, ruxolitinib precursors (54), containing a pyrazole heterocycle with pinacol boronic ester (Bpin) or bromide moieties, only afforded useful yields of remote methylene oxidation products (38% and 33%, 39 and **40**, respectively) in the absence of HBF<sub>4</sub> protonation.

Cyclopentane and cyclohexane carbocycles are common bioisosteres for aromatic rings; however, they are rarely structural starting points in drug discovery due to the difficulty in generating functionalized analogs (2). We investigated Mn(CF<sub>3</sub>-PDP) 1 oxidations of carbocyclic drug candidates of high complexity (BertzCT (48) = 500 to 1,121), previously shown to have greater potency than their aromatic counterparts (Fig. 3). An 11β-hydroxysteroid dehydrogenase inhibitor reported a twofold increase in potency when a benzyl group was exchanged for a cyclopentyl group

(Fig. 3A) (55). Mn(CF<sub>3</sub>-PDP) 1 oxidation of 41, bearing a tetrazole moiety (ca.  $pK_{aH} = -2.7$ ) gave a single remote oxidation product 42 in 41% yield. A dioxo-triazine cathepsin K inhibitor reported a sixfold boost in potency when the N-phenyl substituent was exchanged for a cyclopentyl ring (Fig. 3B) (56). Oxidation of this bioisostere 43 afforded 56% yield of remote ketone \$45 that provides a functional group handle for further diversification. The ketone was diastereoselectively reduced to alcohol 44 followed by deoxyfluorination to afford the monofluorine compound 45 as a single diastereomer.

Exchange of an aromatic ring for a saturated carbocycle introduces new  $C(sp^3)$ -H sites for oxidative metabolism. We hypothesized that the site selectivity of Mn(CF<sub>3</sub>-PDP) 1 C(sp<sup>3</sup>)-H oxidation may correlate with that of promiscuous CYP450 liver enzymes, thereby providing an expedient and preparative way to perform early MetID studies to inform rational drug design. Exchanging the aromatic rings in valdecoxib and celecoxib, both nonsteroidal anti-inflammatories, for cyclopentyl rings afforded bioisosteres, **46** and **48** (Fig. 3 C and D). Notably, whereas monosubstituted isoxazole in a simple substrate was poorly tolerated (Fig. 2A), Mn(CF<sub>3</sub>-PDP) 1 remote oxidation of a trisubstituted isoxazole in 46 furnished ketone \$46 in 43% yield. Similar improvements in yield were observed with pyrazoles, with the trisubstituted pyrazole in 48 affording a single ketone S47 in 73% yield. This underscores how simple model substrates may underpredict functional group tolerance for Mn(CF<sub>3</sub>-PDP) 1 oxidations in complex molecule settings where greater steric and/or electronic influences can impede heterocycle oxidation.

Both 46 and 48 afforded hydroxylated metabolites when incubated with rat liver microsome preparations (Fig. 3 C and D, CI<sub>int</sub> = unscaled intrinsic metabolic clearance (μL/min/mg); rat liver microsomes: 46 CI<sub>int</sub> = 66; 48 CI<sub>int</sub> = 136; for human liver microsome CI<sub>int</sub>, see SI Appendix). LC-MS/MS fragmentation pattern analysis localized hydroxylation to the cyclopentyl ring of 46 and 48 but could not determine the exact site of oxidation. In contrast, preparative late-stage oxidation enabled rapid metabolite ID: Mn(CF<sub>3</sub>-PDP) 1 oxidation products, ketones **S46** and **S47** were reduced to alcohols 47 (d.r. = 9:1) and 49 (d.r. = 2:1), and both sets of diastereomers matched with the primary metabolites by HPLC retention times, exact mass from quadrupole time of flight (QTOF) measurements, and MS-MS fragmentation patterns. Alcohol 49 underwent deoxyfluorination to afford fluorinated diastereomers 50, that showed decreased metabolism in rat liver microsomes (CI<sub>int</sub> 57 µL/min/mg), with metabolism no longer observed on the cyclopentyl ring. In contrast, ketones \$46 and S47 (SI Appendix) and alcohols 47 and 49 were stable to further oxidation ( $CI_{int}$  < 20  $\mu$ L/min/mg), likely due to a decrease in their lipophilicity (57).

A benzimidazole series of hepatitis C NS5B polymerase inhibitors reported an 84-fold boost in potency when an N-phenyl was exchanged for a cyclohexyl substituent (Fig. 3E) (3). Intercepting an ester precursor of the HCV inhibitor 51, HBF<sub>4</sub> protection deactivated the pyridine as well as the benzimidazole functionality toward oxidation. Mn(CF<sub>3</sub>-PDP) 1 oxidation afforded a separable mixture of remote y-alcohol 53 as a single observed diastereomer and δ-ketone **55** in 53% overall yield. Reduction of the ketone followed by hydrolysis of the esters resulted in two alcohol analogs 54 and 56 of the parent inhibitor. Although the compound was relatively stable to metabolism (rat  $CI_{int} = 32 \mu L/min/mg$ ), the major metabolite matched Mn(CF<sub>3</sub>-PDP) 1 generated δ-cis-alcohol 56 by HPLC retention times, exact mass from QTOF measurements, and MS-MS fragmentation patterns.

A series of pyrimidine-based COX-2 inhibitors reported a ninefold boost in potency when the phenyl ring was exchanged for a

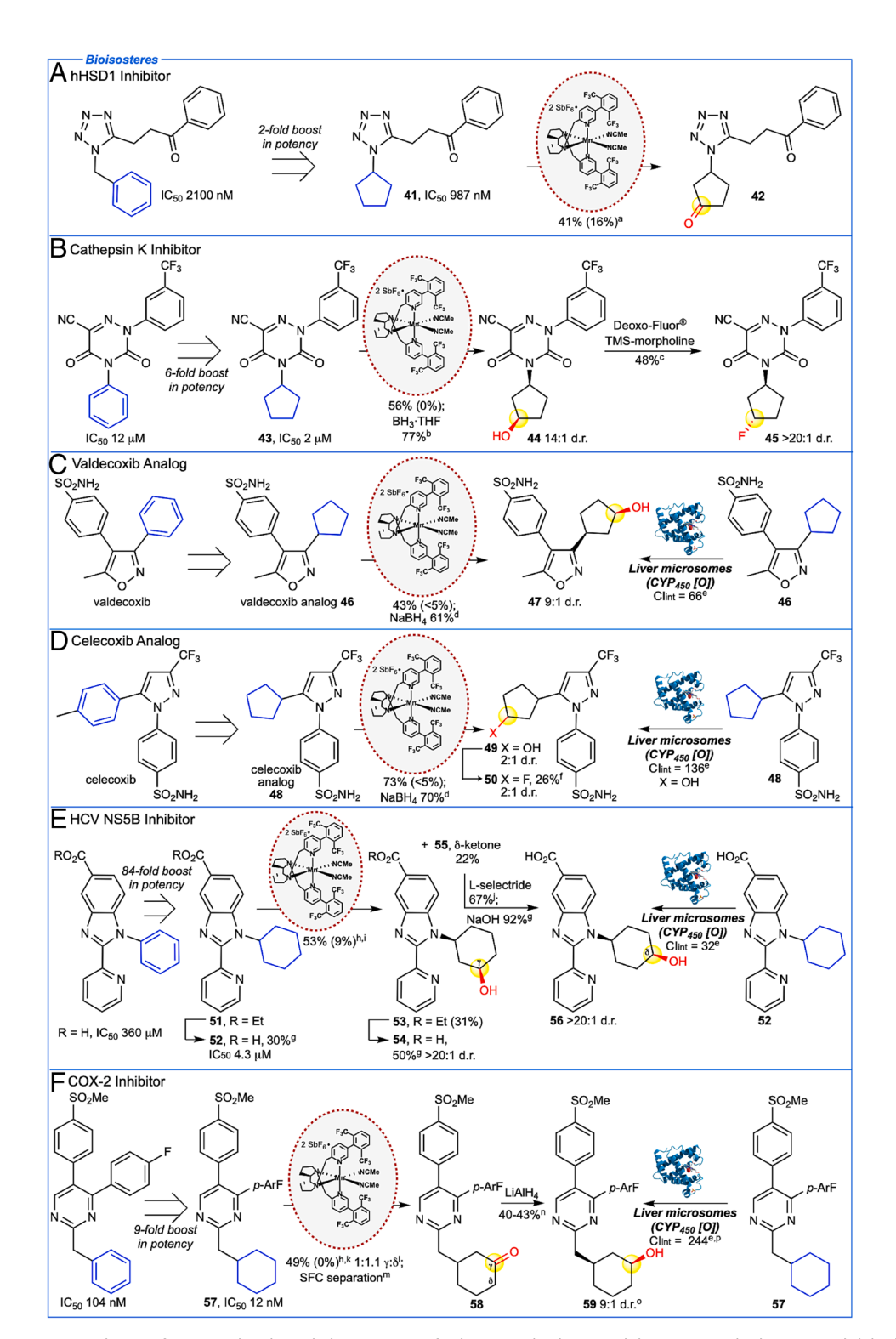


Fig. 3. Mn(CF<sub>3</sub>-PDP) 1 C-H oxidation of saturated carbocycle bioisosteres of *N*-heterocyclic drug candidates. (*A*) 11β-hydroxysteroid dehydrogenase (hHSD1) inhibitor reported a twofold increase in potency for cyclopentyl bioisostere 41 that can be oxidized selectively to give cyclopentanone 42. (*B*) Cathepsin K inhibitor reported a sixfold increase in potency in cyclopentyl bioisostere 43 that can be oxidized selectively and diversified by reduction and deoxyfluorination. (C) Cyclopentyl bioisostere of valdecoxib 46 undergoes selective oxidation and reduction to form alcohol 47 at the same carbon as CYP450 enzymes. (*D*) Cyclopentyl bioisostere of celecoxib 48 undergoes selective oxidation and reduction to form alcohol 49 at the same carbon site as CYP450 enzymes. Fluorination affords 50 that shows reduced metabolism in rat liver microsomes (Cl<sub>int</sub> 57 μL/min/mg) relative to 48. (*E*) Hepatitis C (HCV) inhibitor reported an 84-fold increase in potency in cyclohexyl bioisostere 52. Precursor 51 can be oxidized to form a single diastereomer of γ-alcohol 53 and δ-ketone 55. Reduction of the ketone and hydrolysis forms alcohol 56 at the same carbon site with the same stereochemistry as CYP450 enzymes. (*F*) COX-2 inhibitor reported a ninefold increase in potency in cyclohexyl bioisostere 57 that can be oxidized to give γ- and δ-ketones 58 which can be diversified by reduction to form alcohol 59 at the same carbon site as CYP450 enzymes. Method B is used unless otherwise noted. <sup>8</sup> Method A at 0 °C. <sup>8</sup>BH<sub>3</sub>\*THF (1.1 equiv.) in THF, 0 °C. <sup>9</sup>Deoxo-Fluor<sup>®</sup> (6.0 equiv.), TMS-morpholine (6.0 equiv.), refluxed in CH<sub>2</sub>Cl<sub>2</sub> overnight. <sup>4</sup>NaBH<sub>4</sub> (1.1 equiv.) in MeOH, 60 °C. <sup>8</sup>Unscaled intrinsic clearance in rat liver microsome preparations, μL of compound metabolized per minute per mg of protein. For human liver microsome preparation, see *SI Appendix*. <sup>5</sup>Deoxo-Fluor<sup>®</sup> (6.0 equiv.), TMS-morpholine (6.0 equiv.), refluxed in toluene overnight. <sup>8</sup>2M NaOH (2.7 equiv.) in THF, -78 °C. <sup>8</sup>Modified method A [5 mol% M

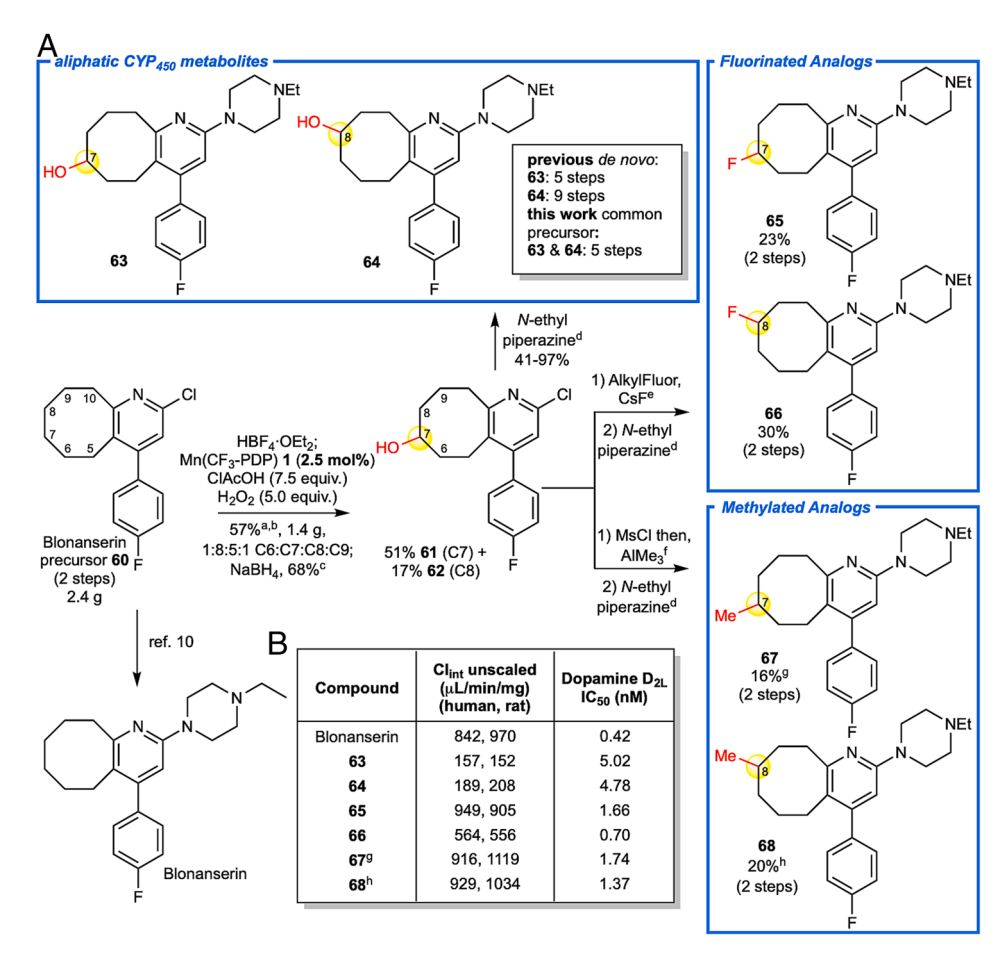


Fig. 4. Streamlining blonanserin metabolite and analog synthesis. (A) Blonanserin precursor 60 was oxidized on a 2.4 g scale with Mn(CF<sub>3</sub>-PDP) 1 to afford 1.4 g of a mixture of ketone products at C7 and C8, known sites of CYP450 metabolism, with minor ketone products observed at C6 and C9. The yield is comparable to that on a 0.3-mmol scale using 10 mol% Mn(CF<sub>3</sub>-PDP)  $\mathbf{1}$  (49% of C7 and C8). Reduction of ketones to alcohols  $\mathbf{61}$  and  $\mathbf{62}$  followed by S<sub>N</sub>Ar cross-coupling afforded known metabolites  $\mathbf{63}$  and  $\mathbf{64}$ . Diversification of alcohols  $\mathbf{61}$  and  $\mathbf{62}$  via deoxyfluorination and oxidative methylation followed by cross-coupling afforded fluorinated (65 and 66) and methylated (67 and 68) analogs, respectively. (B) Compounds from analog library were subjected to metabolism studies to measure intrinsic clearance in rat and human liver microsomes. Measurement of  $IC_{50}$  values of blonanserin and analogs against Dopamine  $D_{2L}$  receptor using a known radioligand binding assay. <sup>a</sup>Nitrogen was HBF<sub>4</sub>·OEt<sub>2</sub> protected, and modified method D was used. <sup>b</sup>C7 and C8 were the major sites of oxidation, C7+C8:C6+C9 = 5.5:1. <sup>c</sup>NaBH<sub>4</sub> (1.1 equiv.) in MeOH. <sup>d</sup>N-ethyl piperazine (15.0 equiv.), KI (1.0 equiv.), heated to 165 °C. <sup>e</sup>AlkylFluor (1.2 equiv.), CsF (5.0 equiv.) generate PhenoFluor in situ as described in ref. 62. Methylation procedure as described in ref. 47 was performed on pure C7 and C8 alcohols. This afforded olefin by-products that were removed via HBF4 OEt2 nitrogen protection then mCPBA (1.6 equiv.) oxidation. g1:1 C7:C6. h2:1 C8:C9.

cyclohexyl ring (Fig. 3F) (58). Mn(CF<sub>3</sub>-PDP) 1 catalysis was applied to both isomeric aromatic series (57 and S43) and afforded a mixture of  $\gamma\text{-}$  and  $\delta\text{-}ketones$  on the cyclohexyl rings in synthetically useful yields (58, 49%  $\gamma$ : $\delta$  = 1:1.1, and \$53/\$54 56%  $\gamma$ : $\delta$  = 1:1.3, see SI Appendix). Whereas simple pyrimidines performed equally well with and without HBF<sub>4</sub> protonation, pyrimidines 57 and S43, with extended  $\pi$ -systems, required protonation to obtain optimal yields (SI Appendix). Following chiral supercritical fluid (SFC) separation of the ketone mixtures, reduction afforded  $\gamma$ -alcohols (+)-59a and (–)-59b and  $\delta$ -alcohol S52 (isomeric series: (+)-S56, (–)-S57, and **\$58**, see *SI Appendix*). COX-2 inhibitor **57** afforded aliphatic hydroxylated metabolites when incubated with either rat or human liver microsome preparations (rat CI<sub>int</sub> = 244; human CI<sub>int</sub> = 223, see SI Appendix) with the major metabolite in both cases matching Mn(CF<sub>3</sub>-PDP) 1 generated compound 59 by HPLC retention times, exact mass from QTOF measurements, and MS-MS fragmentation patterns. The demonstrated ability of Mn(CF<sub>3</sub>-PDP) 1 catalysis to generate the major aliphatic metabolite of a diverse series of N-heterocyclic bioisostere drug analogs supports its broad applicability as a functional mimic of CYP450 enzymes.

Blonanserin, an atypical antipsychotic approved for treatment of schizophrenia in Asia, undergoes extensive oxidative CYP450 metabolism (10, 11). In order to confirm aliphatic oxidation at C7 and C8 on the cyclooctyl ring, independent 5 to 9 step de novo

syntheses were needed. In contrast, a late-stage blonanserin intermediate **60** underwent Mn(CF<sub>3</sub>-PDP) **1** oxidation (2.5 mol%) on a 2.4 g (8.3 mmol) scale to directly furnish 1.4 g of oxidized material (57% yield, Fig. 4A). Analogous to CYP450 enzymes, the major sites of aliphatic oxidation were observed at C7 and C8 (ketones **S59a** and **S59b**, 1.2 g, 48% yield, C7:C8 = 1.6:1) with minor oxidation at C6 and C9 (ketones S59c and S59d, 218 mg, 9% yield, C6:C9 = 1:1.3). The lack of benzylic oxidation can be rationalized by electronic deactivation at C10 due to the protonated pyridine, steric deactivation of C5 by the proximal aryl group, and stereoelectronic deactivation of both sites by torsional strain that is introduced during aromatic radical stabilization (22, 29, 59).

The late-stage oxidation (60, 61) of advanced hydrocarbon precursor 60 on multigram scale afforded sufficient material to synthesize hydroxylated metabolites as well as fluorinated and methylated blonanserin analogs for biological studies (Fig. 4A). Reduction of the C7 and C8 ketones (**S59a** and **S59b**) afford alcohols 61 and 62 followed by S<sub>N</sub>Ar cross-coupling afforded (±)-7-hydroxyl 63 and (±)-8-hydroxyl 64 blonanserin metabolites in a significantly reduced overall step count (11). Deoxyfluorination of alcohols 61 and 62 with in situ generated PhenoFluor (62) and subsequent cross-coupling furnished C7 and C8 fluorinated analogs 65 and 66. Methylation of 61 and 62 using our oxidative methylation protocol (47) afforded C7 and C8 methylated analogs 67 and

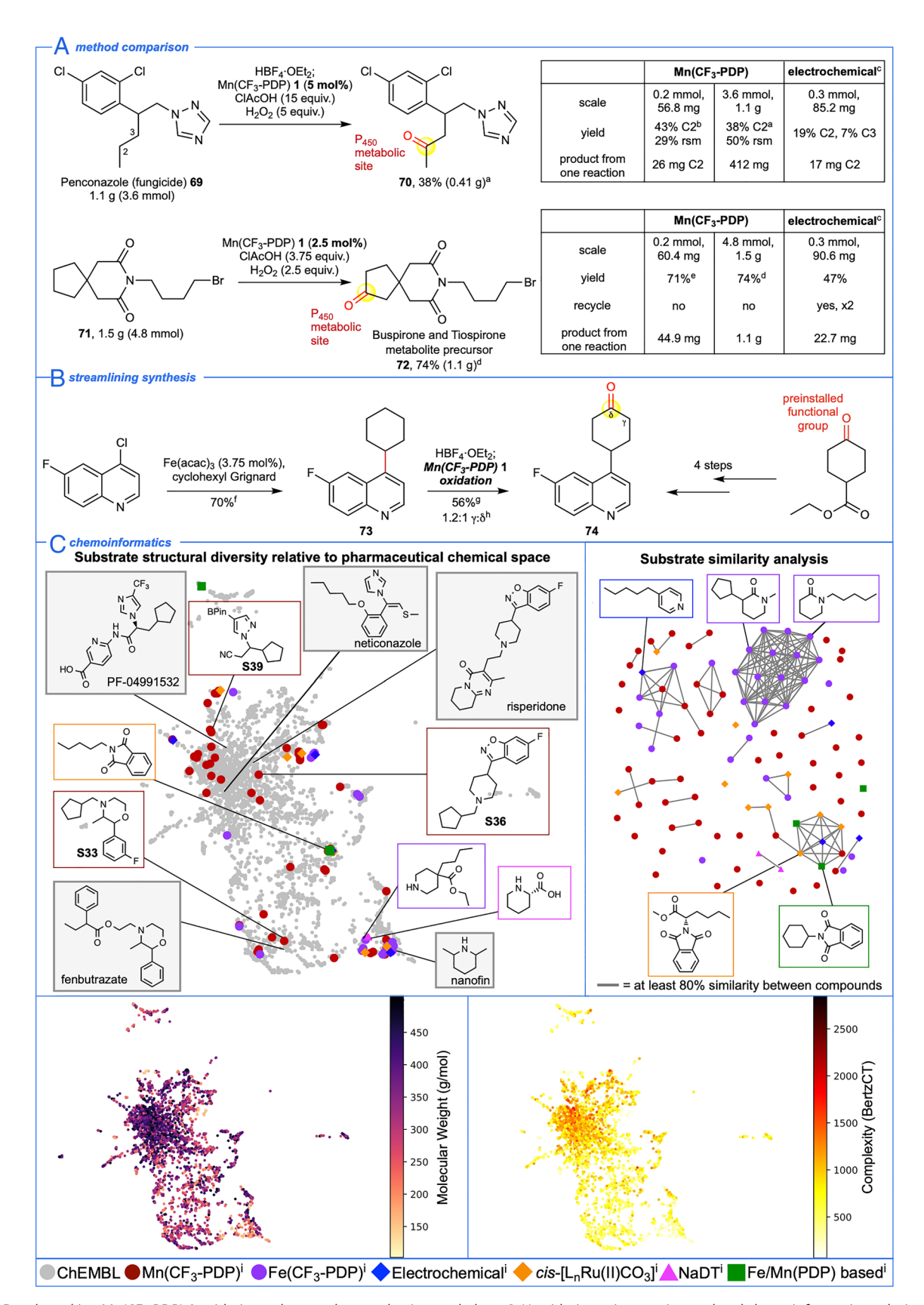


Fig. 5. Benchmarking Mn(CF₃-PDP) 1 oxidation to known chemoselective methylene C–H oxidations via experimental and chemoinformatic analysis. (*A*) Large-scale (1 to 1.5 g) oxidation of **69** and **71** with Mn(CF₃-PDP) 1 at low catalyst loadings (2.5 to 5 mol%) affords known penconazole metabolite **70** and buspirone/tiospirone metabolite precursor **72** in preparative quantities (0.41 to 1.1 g). This compares favorably to previously reported electrochemical oxidations. (*B*) Mn(CF₃-PDP) 1 oxidation enables streamlining synthesis of **74** en route to linrodostat (BMS-986205). (*C*) Chemoinformatic investigation of Mn(CF₃-PDP) 1 and all other methods reporting methylene oxidation in *N*-heterocyclic compounds relative to pharmaceutical chemical space. All examples with ≥15% yield of monoxidized compounds were included. Pyrrolidine, piperidine, and azepane from NaDT (sodium decatungstate) were filtered out due to low molecular weight (<100 g/mol). <sup>a</sup>Nitrogen was HBF₄-OEt₂ protected followed by modified method D at 0 °C. <sup>b</sup>Nitrogen was HBF₄-OEt₂ protected followed by method A. <sup>b</sup>Ratios are statistically corrected. <sup>l</sup>These catalysts can be found in refs. 26, 29, 36–42.

68. Whereas known C7 and C8 metabolites 63 and 64 showed lower rates of metabolism relative to the parent, they also had reduced binding affinity to the human dopamine D<sub>2L</sub> receptor, a known central nervous system target for blonanserin (Fig. 4B). Fluorinated and methylated analogs (65 to 68) retained potency with the C8 fluorinated analog (66) being comparable to that of the parent compound, blonanserin. Although substitution of hydrogen with fluorine or methyl groups at metabolically labile sites is a well-precedented approach for attenuating metabolism (57), blocking aliphatic sites C7 and C8 with these groups did not significantly impact metabolic clearance due to extensive oxidation on the piperazine motif. Collectively, these studies show that Mn(CF<sub>3</sub>-PDP) 1 is a preparative late-stage C-H oxidation catalyst for efficient generation of metabolites and analogs on aliphatic portions of heterocyclic drugs to rapidly inform MetID and SAR studies.

Given the demonstrated capacity of Mn(CF<sub>3</sub>-PDP) 1 catalysis to serve as a preparative mimic of promiscuous CYP450 enzymes, we were interested in evaluating other important metrics such as yield and scale relative to previous state-of-the-art chemical methods used in aliphatic metabolite synthesis (Fig. 5A). Penconazole 69, a widely used fungicide, has monohydroxylated metabolites at C1 and C2 carbons of the propyl side chain (63). Electrochemical oxidation of penconazole 69 on an 85.2 mg scale (0.3 mmol) was reported to afford 17 mg C2 ketone **70** (19%) and 6.3 mg C3 ketone (7%) (38). In contrast, Mn(CF<sub>3</sub>-PDP) 1 (5 mol%) oxidation of penconazole **69** on a 1 g scale (3.6 mmol) afforded 412 mg (1.4 mmol, 38% yield) of C2 oxidized product 70 with 50% rsm. Imide 71 was reported to undergo electrochemical oxidation to afford 22.7 mg (24% yield) of ketone 72, a precursor to the metabolites of buspirone (64) and tiospirone (65), with 64% rsm (38). Recycling of the starting material two times was needed to furnish 44.6 mg of ketone 72 in 47% overall yield. In comparison, Mn(CF<sub>3</sub>-PDP) 1 oxidation (2.5 mol%) of 71 was performed on a 1.5 g (4.8 mmol) scale to afford 1.1 g of ketone 72 (74% yield) in a single reaction. These examples serve to underscore the practical, robust nature of Mn(CF<sub>3</sub>-PDP) 1 catalysis that uses commercial reagents and ambient reaction conditions to directly access gram quantities of metabolites and their precursors. The scalability of the Mn(CF<sub>3</sub>-PDP) 1 oxidation is noteworthy: comparable yields are observed upon 18- to 28-fold increases in scale using 25 to 50% of the standard catalyst loading (10 mol%) relative to the 0.2 to 0.3 mmol reactions (Figs. 4A and 5A). Mn(CF<sub>3</sub>-PDP) 1  $C(sp^3)$ -H oxidation is noteworthy in its

capacity to streamline synthesis of pharmaceuticals and intermediates by connecting late-stage aliphatic oxidation with powerful  $C(sp^2)$ – $C(sp^3)$  cross-coupling (66), currently well precented for unfunctionalized carbocycles (Fig. 5B) (67). The route to linrodostat, an anticancer compound in clinical trials, proceeds through ketone intermediate 74 whose key C-C bond forming step linking the preoxidized cyclohexanone and quinoline fragments required three functional group manipulations (Fig. 1C) (9). In contrast,  $C(sp^2)$ – $C(sp^3)$  cross-coupling (66) linked an unfunctionalized cyclohexane to the quinoline heterocycle (73) followed by Mn(CF<sub>3</sub>-PDP) 1 oxidation to afford  $\gamma$ - and  $\delta$ -ketones 74 in 2 steps, with no functional group manipulations.

Evaluation of heterocycle scope diversity shows that Mn(CF<sub>3</sub>-PDP) 1 methylene oxidation, first reported in 2019 (26), tolerates 14 of the 27 (52%) most frequent heterocycles in FDA-approved drugs (1); this compares favorably to all other methylene C-H oxidation methods reported with similar chemoselectivity from 2015 to 2021 combined (7 out of 27, 26%) (29, 36-42). However, simple heterocycle scope may not correlate to whole molecule drug-likeness; therefore, we sought to evaluate the overall structural diversity of substrates in the context of pharmaceutical chemical space (Fig. 5C) (68, 69). A data set of small-molecule drugs obtained from ChEMBL

(70) was combined with N-heterocyclic molecules successfully oxidized using ours and other representative aliphatic C-H oxidation methods [Mn(CF<sub>3</sub>-PDP) (26) 1, Fe(CF<sub>3</sub>-PDP) (29, 36), electrochemical (37, 38), bis(bipyridine)-ruthenium (39), sodium decatungstate (NaDT) (40), and other Fe/Mn(PDP)-based catalysts (41, 42)]. All of these molecules were filtered based on the presence of N-heterocycles, molecular weight (100 to 500 g/mol),  $\geq 4 \text{ sp}^3$ atoms, and other physical properties (see SI Appendix for details). This resulted in 4,499 molecules for which a topological fingerprint was calculated using RDKit (71) that quantitatively describes atom connectivity across the entire molecule. Uniform Manifold Approximation and Projection (UMAP) (72), a reliable technique that provides a low dimensional representation of multidimensional data, was used to visualize substrates of the C-H oxidation methods (colored) before and after Mn(CF<sub>3</sub>-PDP) 1 compared to drug-like chemical space (gray) (Figs. 1E and 5C). Substrates from previous methods (many colors), including those reported with our Fe(CF<sub>3</sub>-PDP) catalysis (purple) (29, 36), tend to cluster tightly in sparsely occupied regions of pharmaceutical space (gray). Substrates for Mn(CF<sub>3</sub>-PDP) 1 oxidations (red), all obtained via de novo synthesis or from readily available commercial sources (see SI Appendix for details), are well dispersed and reside in both previously reported and novel, densely occupied regions of pharmaceutical chemical space (gray). Gradient plot analyses of the chemical space provided by UMAP indicate that the novel regions contain higher-molecular-weight and higher-complexity pharmaceuticals. For example, substrates \$33, \$36, and \$39 share heterocyclic cores and whole molecule drug-like motifs with complex pharmaceuticals fenbutrazate, risperidone, and PF-04991532. In contrast, piperidine substrates from previous methods share chemical space with fragment-sized drugs such as nanofin. Consistent with this, a plot that connects compounds using a Tanimoto coefficient (73) shows nearly all substrates from previous reports share ≥80% structural similarity with at least one other molecule, whereas Mn(CF<sub>3</sub>-PDP) 1 substrates show limited connectivity indicating high structural diversity. For example, the largest cluster is composed of small aliphatic amides that make up 54% of all N-heterocyclic molecules oxidized using Fe(CF3-PDP) catalysis. The second largest cluster consists of phthalimide heterocycles, which have low representation in drugs, but comprise 42% of substrates oxidized with non-CF<sub>3</sub>-PDP methods. Pharmaceutical space that is not represented by any of the methods (i.e., neticonazole) serves to highlight underdeveloped areas in chemoselective aliphatic C-H oxidations such as tolerance for electron-rich aromatic rings and sulfur functionality.

### **Conclusions**

A comprehensive evaluation of commercial Mn(CF<sub>3</sub>-PDP) 1 methylene C-H oxidation catalysis reveals noteworthy scalability and chemoselectivity for methylene oxidation in the presence of oxidatively labile N-heterocycles. A chemoinformatic analysis of the scope supports Mn(CF<sub>3</sub>-PDP) 1 catalysis affords a significant expansion in the structural diversity accessible by chemical C-H oxidation methods relative to pharmaceutical chemical space. This expanded scope enabled the comparison of Mn(CF<sub>3</sub>-PDP) 1 site-selectivities with those of liver CYP450 enzymes in the late stage oxidation of drug molecules, leading to the powerful conclusion that small molecule catalysis is capable of mimicking aliphatic site-selectivities of such promiscuous enzymes. Collectively, the preparative nature of Mn(CF<sub>3</sub>-PDP) 1 smallmolecule catalysis combined with its chemo- and site-selectivity opens the door for its use as a functional mimic of liver CYP450 enzymes to rapidly inform MetID and SAR studies in pharmacology.

#### **Materials and Methods**

General Procedure for HBF4 Protection/Deprotection. To a flame-dried 40-mL vial with a magnetic stir bar were added substrate (0.3 mmol, 1.0 equiv.) and anhydrous CH<sub>2</sub>Cl<sub>2</sub> (1.2 mL, 0.25 M). The vial was flushed with an N<sub>2</sub> stream and then cooled to 0 °C. HBF<sub>4</sub>•OEt<sub>2</sub> (45 µL, 1.1 equiv.) was added dropwise via a syringe, and the reaction was allowed to stir at 0 °C for 30 min and then warmed to room temperature and stirred for an additional 1 h. The reaction was concentrated in vacuo and left on high vacuum overnight (12 to 24 h). Resultant HBF<sub>4</sub> salts were used as substrates.

HBF4 deprotection. After completion of the oxidation reaction, the following workup was done. The reaction was warmed to room temperature and concentrated in vacuo to a minimum amount of solvent (CAUTION: Do not concentrate to dryness due to residual H<sub>2</sub>O<sub>2</sub>). The reaction was diluted with DCM (10 mL), basified with 3 M NaOH (10 mL), and stirred vigorously for 20 min. The resulting solution was poured into 3 M NaOH (30 mL) and extracted with DCM (3  $\times$  20 mL). The combined organic layer was washed with brine (1 × 60 mL) and then dried with Na<sub>2</sub>SO<sub>4</sub>. The filtrate was concentrated and purified by flash column chromatography on silica gel.

General Oxidation Procedure Method A (Double Slow Addition of Catalyst and Oxidant). A 40-mL vial was charged with substrate (0.3 mmol, 1.0 equiv.), CICH<sub>2</sub>CO<sub>2</sub>H (CIAcOH, 425 mg, 4.5 mmol, 15.0 equiv.), and a stir bar. Acetonitrile (MeCN, 0.6 mL, 0.5 M) was added along the wall to ensure that all compounds were washed beneath the solvent level and the vial was sealed with a screw cap fitted with a PTFE/Silicone septum. The vial was cooled to -36 °C with 1,2-dichloroethane/dry ice bath or to 0 °C with ice/water bath. A solution of the Mn(CF3-PDP) 1 catalyst (40.7 mg, 0.03 mmol, 10 mol%) in MeCN (0.375 mL, 0.083 M) was taken up in a 1.0 mL syringe. Mn(CF3PDP) 1 is commonly known as the White-Gormisky-Zhao catalyst and is commercial from Strem and the chloride precursor, which must undergo silver hexafluoroantimonate metathesis prior to use, is commercial from J&K Scientific. A few drops of this solution were added to the reaction. A 10-mL syringe was filled with a solution of  $H_2O_2$  (204 mg, 3.0 mmol, 10.0 equiv., 50% wt. in  $H_2O_2$  purchased from Sigma-Aldrich) in MeCN (3.75 mL, 0.8 M). Both syringes were fitted with 25G needles and loaded in a syringe pump resulting in a simultaneous addition of catalyst and oxidant solutions over 3 h while the reaction vial was maintained at the corresponding temperature (1.25 mL/h addition rate set for the H<sub>2</sub>O<sub>2</sub> syringe; 0.125 mL/h for the catalyst syringe). Upon completion, the reaction was warmed to room temperature and concentrated in vacuo to a minimum amount of solvent (CAUTION: Do not concentrate to dryness due to residual H<sub>2</sub>O<sub>2</sub>). When HBF<sub>4</sub> protection was used, NaOH workup was performed (HBF<sub>4</sub> deprotection).

NaHCO<sub>3</sub> workup. When no HBF<sub>4</sub> protection was used, the residue was dissolved in ~20 mL DCM and washed with 20 mL sat. NaHCO<sub>3</sub> solution (CAUTION: CO<sub>2</sub> was released) to remove CIAcOH. The aqueous layer was extracted with DCM (2 × 15 mL), and the combined organic layer was dried with Na<sub>2</sub>SO<sub>4</sub>. When method A is used for tertiary oxidation, the following changes are made: Mn(PDP) 2 (27.9 mg, 0.03 mmol, 10 mol%) with H<sub>2</sub>O<sub>2</sub> (102 mg, 1.5 mmol, 5.0 equiv., 50% wt. in H<sub>2</sub>O, purchased from Sigma-Aldrich), and the vial is cooled and maintained at -36 °C for the course of the reaction.

General Oxidation Procedure Method B (Single Slow Addition of Oxidant). A 40-mL vial was charged with substrate (0.3 mmol, 1.0 equiv.), Mn(CF<sub>3</sub>-PDP) 1 catalyst (40.7 mg, 0.03 mmol, 10 mol%), ClAcOH (425 mg, 4.5 mmol, 15.0 equiv.), and a stir bar. Acetonitrile (MeCN, 0.6 mL, 0.5 M) was added along the wall as in method A. The vial was cooled to 0 °C with an ice/water bath. A separate solution of H<sub>2</sub>O<sub>2</sub> (204 mg, 3.0 mmol, 10.0 equiv., 50% wt. in H<sub>2</sub>O) in MeCN (3.75 mL, 0.8 M) was loaded into a 10-mL syringe fitted with a 25G needle and was added dropwise to the stirring reaction over 3 h via a syringe pump (1.25 mL/h addition rate) while the reaction vial was maintained at the corresponding temperature. Upon completion, the reaction mixture was treated as in method A. When method B is used for tertiary oxidation, the following changes are made: Mn(PDP) **2** (27.9 mg, 0.03 mmol, 10 mol%) with  $H_2O_2$  (102 mg, 1.5 mmol, 5.0 equiv., 50% wt. in H<sub>2</sub>O, purchased from Sigma-Aldrich), and the vial is cooled and maintained at -36 °C for the course of the reaction.

Method C (Iterative Catalyst Addition, Slow Addition Oxidant). This protocol was used when method B gave low conversion and method A gave low rsm. A 40-mL vial was charged with substrate (0.3 mmol, 1.0 equiv.), Mn(CF<sub>3</sub>-PDP) 1 catalyst (20.3 mg, 0.015 mmol, 5 mol%), CIAcOH (425 mg, 4.5 mmol, 15.0 equiv.), and a stir bar.

Acetonitrile (MeCN, 0.6 mL, 0.5 M) was added along the wall as in method A. The vial was cooled to -36 °C or 0 °C. A separate solution of  $H_2O_2$  (204 mg, 3.0 mmol, 10.0 equiv., 50% wt. in H<sub>2</sub>O) in MeCN (3.75 mL, 0.8 M) was loaded into a 10-mL syringe fitted with a 25-G needle and was added dropwise to the stirring reaction over 3 h via a syringe pump (1.25 mL/h addition rate) while the reaction vial was maintained at the corresponding temperature. At 1.5 h, an additional 5 mol% Mn(CF<sub>3</sub>-PDP) 1 catalyst (20.3 mg, 0.015 mmol in 0.1 mL MeCN) was added dropwise to the reaction. Upon completion, the reaction mixture was treated as in method A. If low conversion is observed, the catalyst can be added three times at 5 mol% (0.015 mmol in 0.1 mL MeCN) with addition done every hour. When method C is used for tertiary oxidation, the following changes are made: Mn(PDP) 2 (14.0 mg, 0.015 mmol, 5 mol%) with  $H_2O_2$  (102 mg, 1.5 mmol, 5.0 equiv., 50% wt. in  $H_2O_3$ ), and the vial is cooled and maintained at -36 °C bath for the course of the reaction.

Method D (Low Catalyst Loading Procedure). A 40-mL vial was charged with substrate (0.3 mmol, 1.0 equiv.), CIAcOH (107 mg, 1.13 mmol, 3.75 equiv.), and a stir bar. Acetonitrile (MeCN, 1.0 mL, 0.3 M) was added along the wall as in method A. The vial was cooled to 0 °C. A 1.0-mL syringe was filled with a solution of the Mn(CF<sub>3</sub>-PDP) 1 catalyst (10.2 mg, 0.0075 mmol, 2.5 mol%) in MeCN (0.625 mL, 0.012 M). A few drops of this solution were added to the reaction. A 10-mL syringe was filled with a solution of H<sub>2</sub>O<sub>2</sub> (51  ${
m mg}$ , 0.75  ${
m mmol}$ , 2.5  ${
m equiv.}$ , 50%  ${
m wt.}$  in  ${
m H_2O}$ ) in MeCN (6.25  ${
m mL}$ , 0.12  ${
m M}$ ). Both syringes were fitted with 25G needles and loaded in a syringe pump resulting in a simultaneous addition of catalyst and oxidant solutions over 3 h while the reaction vial was maintained at 0 °C (2.083 mL/h addition rate set for the H<sub>2</sub>O<sub>2</sub> syringe; 0.208 mL/h for the catalyst syringe). Upon completion, the reaction mixture was treated as in method A. If low conversion was observed, amounts of reagents were altered: Mn(CF<sub>3</sub>-PDP) 1 (2.5 or 5 mol%), ClAcOH (3.75, 5, 7.5, or 15 equiv.),  $H_2O_2$  (2.5 or 5 equiv.). For large-scale reactions (3.6 to 8.3 mmol), oxidant/MeCN solution was loaded into multiple syringes, and upon depletion of oxidant solution, the next syringe with oxidant was loaded into the syringe pump and addition continued.

Data, Materials, and Software Availability. All data and scripts for the chemoinformatics section are available at the Github repository: https://github. com/WhiteGroupUIUC/Mn-CF3PDP-Chemoinformatics (74). All other data are included in the article and/or SI Appendix.

**ACKNOWLEDGMENTS.** Financial support for this work was provided by the National Institute of General Medical Sciences (NIGMS) Maximizing Investigators' Research Award (MIRA R35GM122525) and from a grant from Merck Sharp & Dohme LLC, a subsidiary of Merck & Co., Inc., Rahway, NJ, USA, to study metabolite synthesis. We thank the Molecule Maker Lab Institute (An Al Research Institutes program supported by the NSF, under award no. 2019897) for support for chemoinformatic analysis. Any opinions, findings, and conclusions or recommendations expressed in this material are those of the authors and do not necessarily reflect those of the NIGMS or the NSF. J.K., Associate Professor at Incheon National University, acknowledges the Fulbright Visiting Scholar Program from the Korean-American Educational Commission, funded by the US and Korean governments. We thank L. Zhu and the University of Illinois School of Chemical Science NMR laboratory for assistance with NMR spectroscopic analysis, Z. Firestein for checking the procedure in Fig. 2, compound 12, and J. Wolf for substrate synthesis. We thank Ron Ferguson (Merck & Co., Inc., Rahway, NJ, USA) for assistance with prep-HPLC purification of compounds 58 and \$53/\$54, Kristina McNab (Merck & Co., Inc., Rahway, NJ, USA) for assistance with compound registration and distribution to assays, Scott Borges (Merck & Co., Inc., Rahway, NJ, USA) for assistance with purification of compounds 58 and S53/S54, Dr. Peter Nizner (Merck & Co., Inc., Rahway, NJ, USA) for assistance with obtaining Blonanserin D<sub>21</sub> binding assay data, and Richard W. Gundersdorf (Merck & Co., Inc., Rahway, NJ, USA) for assistance with metabolite ID studies and analyses. We thank Prof. Tobias Ritter for helpful discussions on deoxyfluorination. The Bruker 500-Mz NMR spectrometer was obtained with the financial support of the Roy J. Carver Charitable Trust, Muscatine, IA, USA.

Author affiliations:  $^{\rm a}$ Department of Chemistry, Roger Adams Laboratory, University of Illinois, Urbana, IL 61801; and  $^{\rm b}$ Department of Discovery Chemistry, Merck & Co., Inc., Rahway, NJ 07065

- E. Vitaku, D. T. Smith, J. T. Njardarson, Analysis of the structural diversity, substitution patterns, and frequency of nitrogen heterocycles among U.S. FDA approved pharmaceuticals. J. Med. Chem. 57, 10257-10274 (2014).
- M. A. M. Subbaiah, N. A. Meanwell, Bioisosteres of the phenyl ring: Recent strategic applications in lead optimization and drug design. J. Med. Chem. 64, 14046-14128 (2021).
- P. L. Beaulieu et al., Non-nucleoside inhibitors of the hepatitis C virus NS5B polymerase: Discovery and preliminary SAR of benzimidazole derivatives. Bioorg. Med. Chem. Lett. 14, 119-124 (2004).
- K. B. Teuscher et al., Discovery of potent orally bioavailable WD repeat domain 5 (WDR5) inhibitors using a pharmacophore-based optimization. J. Med. Chem. 65, 6287-6312 (2022).
- J. Genovino, D. Sames, L. G. Hamann, B. B. Touré, Accessing drug metabolites via transitionmetal catalyzed C-H oxidation: The liver as synthetic inspiration. Angew. Chem. Int. Ed. Engl. 55, 14218-14238 (2016).
- A. M. Sawayama et al., A panel of cytochrome P450 BM3 variants to produce drug metabolites and diversify lead compounds. Chem. Eur. J. 15, 11723-11729 (2009).
- R. Slavik, J.-U. Peters, R. Giger, M. Bürkler, E. Bald, Synthesis of potential drug metabolites by a modified udenfriend reaction. Tetrahedron Lett. 52, 749-752 (2011).
- T. Cernak, K. D. Dykstra, S. Tyagarajan, P. Vachal, S. W. Krska, The medicinal chemist's toolbox for late stage functionalization of drug-like molecules. Chem. Soc. Rev. 45, 546-576 (2016).
- K. J. Fraunhoffer et al., Rapid development of a commercial process for linrodostat, an Indoleamine 2,3-Dioxygenase (IDO) inhibitor. Org. Process Res. Dev. 23, 2482-2498 (2019).
- K. Sudarshan Rao, K. Nageswara Rao, T. Uma Sankara Sastry, P. Muralikrishna, A. Jayashree, An investigation into formation of impurities during synthesis of blonanserin. Chem. Asian J. 26, 5928-5930 (2014).
- 11. T. Ochi et al., Syntheses and properties of the major hydroxy metabolites in humans of blonanserin AD-5423, a novel antipsychotic agent. Bioorg. Med. Chem. Lett. 15, 1055-1059 (2005).
- N. F. Gol'dshleger, V. V. Es'Kova, A. E. Shilov, Activation of saturated hydrocarbons. Deuterium hydrogen exchange in solutions of transition metal complexes. Zh. Fiz. Khim. (Engl. Transl.) 46, 785-786 (1972).
- 13. J. T. Groves, T. E. Nemo, Aliphatic hydroxylation catalyzed by iron porphyrin complexes. J. Am. Chem. Soc. 105, 6243-6248 (1983).
- S. Belvedere, R. Breslow, Regioselective oxidation of steroids by a manganese porphyrin carrying metal coordinating groups. Bioorg. Chem. 29, 321-331 (2001).
- T. Okuno, S. Ito, S. Ohba, Y. Nishida, μ-Oxo bridged diiron(III) complexes and hydrogen peroxide: Oxygenation and catalase-like activities. J. Chem. Soc. Dalton Trans., 3547-3551 (1997).
- K. Chen, L. Que Jr., Evidence for the participation of a high-valent iron-oxo species in stereospecific alkane hydroxylation by a non-heme iron catalyst. Chem. Commun., 1375-1376 (1999).
- 17. P. R. Ortiz de Montellano, J. J. De Voss, "Substrate oxidation by cytochrome P450 enzymes" in Cytochrome P450: Structure, Mechanism, and Biochemistry, P. R. Ortiz de Montellano, Ed. (Klumer Academic/Plenum Publishers, 2005), pp. 183-246.
- C. J. C. Whitehouse, S. G. Bell, L.-L. Wong, P450<sub>BM3</sub> (CYP102A1): Connecting the dots. *Chem. Soc.* Rev. 41, 1218-1260 (2012).
- 19. M. A. Bigi, S. A. Reed, M. C. White, Diverting non-haem iron catalysed aliphatic C-H hydroxylations towards desaturations. Nat. Chem. 3, 216-222 (2011).
- W. N. Oloo, L. Que Jr., Bioinspired nonheme iron catalysts for C-H and C=C bond oxidation:
- Insights into the nature of the metal-based oxidants. Acc. Chem. Res. 48, 2612-2621 (2015). M. S. Chen, M. C. White, A predictably selective aliphatic C-H oxidation reaction for complex
- molecule synthesis. Science 318, 783-787 (2007). M. S. Chen, M. C. White, Combined effects on selectivity in Fe-catalyzed methylene oxidation.
- Science 327, 566-571 (2010). 23. P. E. Gormisky, M. C. White, Catalyst-controlled aliphatic C-H oxidations with a predictive model for
- site-selectivity. J. Am. Chem. Soc. 135, 14052-14055 (2013). M. C. White, J. Zhao, Aliphatic C-H oxidations for late-stage functionalization. J. Am. Chem. Soc. 140,
- 13988-14009 (2018). 25. D. C. Blakemore et al., Organic synthesis provides opportunities to transform drug discovery. Nat.
- Chem. 10, 383-394 (2018). J. Zhao, T. Nanjo, E. C. de Lucca Jr., M. C. White, Chemoselective methylene oxidation in aromatic
- molecules. Nat. Chem. 11, 213-221 (2019). R. V. Ottenbacher, D. G. Samsonenko, E. P. Talsi, K. P. Bryliakov, Highly efficient, regioselective, and
- stereospecific oxidation of aliphatic C-H groups with H<sub>2</sub>O<sub>2</sub>, catalyzed by aminopyridine manganese complexes. Org. Lett. 14, 4310-4313 (2012).
- R. K. Chambers, J. Zhao, C. P. Delaney, M. C. White, Chemoselective tertiary C-H hydroxylation for late-stage functionalization with Mn(PDP)/chloroacetic acid catalysis. Adv. Synth. Catal. 362, 417-423 (2020).
- J. M. Howell, K. Feng, J. R. Clark, L. J. Trzepkowski, M. C. White, Remote oxidation of aliphatic C-H bonds in nitrogen-containing molecules. J. Am. Chem. Soc. 137, 14590-14593 (2015).
- G. Asensio, M. E. González-Núñez, C. B. Bernardini, R. Mello, W. Adam, Regioselective oxyfunctionalization of unactivated tertiary and secondary C-H bonds of alkylamines by Methyl(trifluoromethyl)dioxirane in acid medium. J. Am. Chem. Soc. 115, 7250-7253 (1993).
- 31. J. B. C. Mack, J. D. Gipson, J. Du Bois, M. S. Sigman, Ruthenium-catalyzed C-H hydroxylation in aqueous acid enables selective functionalization of amine derivatives. J. Am. Chem. Soc. 139, 9503-9506 (2017).
- V. Dantignana et al., Chemoselective aliphatic C-H bond oxidation enabled by polarity reversal. ACS Cent. Sci. 3, 1350-1358 (2017).
- P. L. Hahn, J. M. Lowe, Y. Xu, K. L. Burns, M. K. Hilinski, Amine organocatalysis of remote, chemoselective C(sp<sup>3</sup>)-H hydroxylation. ACS Catal. 12, 4302-4309 (2022).
- J. Chen et al., Hydrogen bonding-assisted and nonheme manganese-catalyzed remote hydroxylation of C-H bonds in nitrogen-containing molecules. J. Am. Chem. Soc. 145, 5456-5466 (2023).
- E. Gaster, S. Kozuch, D. Pappo, Selective aerobic oxidation of methylarenes to benzaldehydes catalyzed by N-Hydroxyphthalimide and Cobalt(II) acetate in hexafluoropropan-2-ol. Angew. Chem. Int. Ed. Engl. 56, 5912-5915 (2017).

- 36. T. Nanjo, E. C. de Lucca Jr., M. C. White, Remote, late-stage oxidation of aliphatic C-H bonds in amide-containing molecules. J. Am. Chem. Soc. 139, 14586-14591 (2017).
- Y. Kawamata et al., Scalable, electrochemical oxidation of unactivated C-H bonds. J. Am. Chem. Soc. 139. 7448-7451 (2017).
- M. Saito et al., N-Ammonium ylide mediators for electrochemical C-H oxidation. J. Am. Chem. Soc. 143, 7859-7867 (2021).
- 39. J. D. Griffin, D. B. Vogt, J. Du Bois, M. S. Sigman, Mechanistic guidance leads to enhanced siteselectivity in C-H oxidation reactions catalyzed by ruthenium bis(Bipyridine) complexes. ACS Catal. **11**, 10479-10486 (2021).
- D. M. Schultz *et al.*, Oxyfunctionalization of the remote C–H bonds of aliphatic amines by decatungstate photocatalysis. *Angew. Chem. Int. Ed. Engl.* **56**, 15274–15278 (2017).
- M. Milan, M. Bietti, M. Costas, Highly enantioselective oxidation of nonactivated aliphatic C-H bonds with hydrogen peroxide catalyzed by manganese complexes. ACS Cent. Sci. 3, 196-204
- M. Borrell, S. Gil-Caballero, M. Bietti, M. Costas, Site-selective and product chemoselective aliphatic C-H bond hydroxylation of polyhydroxylated substrates. ACS Catal. 10, 4702-4709 (2020).
- J. Zhou et al., Syntheses of 4-(Heteroaryl)cyclohexanones via palladium-catalyzed ester α-arylation and decarboxylation. J. Org. Chem. 82, 9851-9858 (2017).
- J. A. Joule, K. Mills, G. F. Smith, Heterocyclic Chemistry (Chapman & Hall, ed. 3, 1995).
- P. Lassalas et al., Structure property relationships of carboxylic acid isosteres. J. Med. Chem. 59, 3183-3203 (2016).
- F. Hu, M. Szostak, Recent developments in the synthesis and reactivity of isoxazoles: Metal catalysis and beyond. Adv. Synth. Catal. 357, 2583-2614 (2015).
- K. Feng et al., Late-stage oxidative C(sp3)-H methylation. Nature 580, 621-627 (2020).
- S. H. Bertz, The first general index of molecular complexity. J. Am. Chem. Soc. 12, 3599-3601 48. (1981).
- J. T. Madak et al., Design, synthesis, and biological evaluation of 4-quinoline carboxylic acids as inhibitors of dihydroorotate dehydrogenase. J. Med. Chem. 61, 5162-5186 (2018).
- B. E. Blough, R. Rothman, A. Landavazo, K. M. Page, A. M. Decker, "Phenylmorpholines and analogues thereof." US Patent No. 2013/0203752 A1, 8 August 2013. 50
- K. P. Rakesh, C. S. Shantharam, M. B. Sridhara, H. M. Manukumar, H.-L. Qin, Benzisoxazole: A privileged scaffold for medicinal chemistry. Med. Chem. Commun. 8, 2023-2039 (2017).
- R. Sarabu et al., Discovery of piragliatin-First glucokinase activator studied in type 2 diabetic patients. J. Med. Chem. 55, 7021-7036 (2012).
- T. R. Bailey et al., N-(3,3a,4,4a,5,5a,6,6a-octahydro-1,3-dioxo-4,6-ethenocycloprop[f]isoindol-2-(1H)-yl)carboxamides: Identification of novel orthopoxvirus egress inhibitors. J. Med. Chem. 50,
- J. Zhou et al., "Processes for preparing JAK inhibitors and related intermediate compounds." US Patent No. 8,410,265 B2, 2 April 2013.
- S. P. Webster et al., Modulation of 11β-hydroxysteroid dehydrogenase type 1 activity by 1,5-Substituted 1H-Tetrazoles. Bioorg. Med. Chem. Lett. 20, 3265–3271 (2010).
- 56. Z. Rankovic et al., Dioxo-triazines as a novel series of cathepsin K inhibitors. Bioorg. Med. Chem. Lett. 20, 1488-1490 (2010).
- A. F. Stepan, V. Mascitti, K. Beaumont, A. S. Kalgutkar, Metabolism-guided drug design. Med. Chem. Commun. 4, 631-652 (2013).
- P. J. Beswick et al., Identification and optimisation of a novel series of pyrimidine based cyclooxygenase-2 (COX-2) inhibitors. Utilisation of a biotransformation approach. Bioorg. Med. Chem. Lett. 19, 4509-4514 (2009).
- R. B. Miller, C. G. Gutierrez, Synthesis of 9,9-dimethyl-2-methoxy-5-benzosuberone. An unexpected failure of benzylic oxidation. *J. Org. Chem.* **43**, 1569–1573 (1978).
- E. M. Stang, M. C. White, Total synthesis and study of 6-deoxyerythronolide B by late-stage C-H oxidation. Nat. Chem. 1, 547-551 (2009).
- K. J. Fraunhoffer, D. A. Bachovchin, M. C. White, Hydrocarbon oxidation vs C-C bond-forming approaches for efficient syntheses of oxygenated molecules. Org. Lett. 7, 223-226 (2005).
- N. W. Goldberg, X. Shen, J. Li, T. Ritter, AlkylFluor: Deoxyfluorination of alcohols. Org. Lett. 18, 6102-6104 (2016).
- R. Mercadante, E. Polledri, S. Scurati, A. Moretto, S. Fustinoni, Identification of metabolites of the fungicide penconazole in human urine. Chem. Res. Toxicol. 29, 1179-1186 (2016).
- M. Zhu et al., Cytochrome P450 3A-mediated metabolism of buspirone in human liver microsomes. Drug Metab. Dispos. 33, 500-507 (2005).
- J. A. Cipollina et al., Synthesis and biological activity of the putative metabolites of the atypical antipsychotic agent tiospirone. J. Med. Chem. 34, 3316-3328 (1991).
- S. Malhotra, P. S. Seng, S. G. Koenig, A. J. Deese, K. A. Ford, Chemoselective  $sp^2$ - $sp^3$  cross-couplings: Iron-catalyzed alkyl transfer to dihaloaromatics. Org. Lett. 15, 3698-3701 (2013).
- A. W. Dombrowski et al., Expanding the medicinal chemist toolbox: Comparing seven C(sp<sup>2</sup>)-C(sp<sup>3</sup>) cross-coupling methods by library synthesis. ACS Med. Chem. Lett. 11, 597-604 (2020).
- K. D. Collins, F. Glorius, A robustness screen for the rapid assessment of chemical reactions. Nat. Chem. 5, 597-601 (2013).
- P. S. Kutchukian *et al.*, Chemistry informer libraries: A chemoinformatics enabled approach to evaluate and advance synthetic methods. *Chem. Sci.* **7**, 2604–2613 (2016).
- 70. A. Gaulton et al., The ChEMBL database in 2017. Nucleic Acids Res. 45, D945-D954 (2017).
- RDKit: Open-source chemoinformatics software. https://www.rdkit.org. Accessed 19 October 2022.
   L. McInnes, J. Healy, J. Melville, UMAP: Uniform manifold approximation and projection for
- dimension reduction. arXiv [Preprint] (2020). https://doi.org/10.48550/arXiv.1802.03426 (Accessed 19 October 2022).
- T. Sander, J. Freyss, M. von Korff, C. Rufener, DataWarrior: An open-source program for chemistry aware data visualization and analysis. J. Chem. Inf. Model. 55, 460-473 (2015).
- R. K. Chambers et al., Data from "A preparative small-molecule mimic of liver CYP450 enzymes in the aliphatic C-H oxidation of carbocyclic N-heterocycles." Github. https://github.com/ WhiteGroupUIUC/Mn-CF3PDP-Chemoinformatics. Deposited 6 January 2023.